Proceedings of Symposium on Ultrasonic Electronics, Vol. 37 (2016)
16-18 November, 2016

Evaluation of abdominal sound speed tomographic image using regularized ART algorithm

正則化 ART アルゴリズムを用いた腹部音速トモグラフィ画像の性能評価

Akira Yamada†, Kensuke Kawai, and Tomohiro Kurokawa, (Bio-Appl. Sys. Eng., Tokyo Univ. of A&T)
山田 晃†, 河井健輔, 黒川智大 (東京農工大学)

1. Introduction

Studies have ever been made for the realization of the abdominal visceral fat cross-sectional inspection based on the ultrasonic tomography method. [1,2,3] The technique is based on the sound wave travel time data observed by mechanically scanning the ultrasound transmitter and receiver pairs on the abdominal circumference. It is intended to reproduce the abdominal sectional sound speed image information. The method has difficulty in that the number of observation data is extremely small compared to the number of pixels in the image. Moreover, part of the data passing through the spine is missing. It is necessary to encounter the ill-conditioned incomplete tomography problem. In this study, we propose a regularized ART (Algebraic Reconstruction Technique) algorithm to address the problem. In addition, examinations are carried out to demonstrate the validity of the proposed method.

2. Principle and method

2.1 Relationship between measured travel time and objective sound speed distribution

We assume that sound wave travel time T are measured between a facing transmitter and receiver around the abdominal cross-section medium with sound speed $c(x,y)$. Aside from this, background travel time T_0 are prepared corresponding to the data transmitted through the medium with uniform sound speed c_0. The transmitter and receiver are moved to multiple points on the body surface for the measurement of the travel time T_i of the sound wave propagated along the path l_i (i=1,..,M). We define the time lag between T_j and T_0 as $\tau_i=T_i-T_0$, and the inverse sound speed difference between the target and background medium as $f=1/c-1/c_0$. Then, the time lag τ_i along the i-th path is represented as a path integration of the object f as,

$$\tau_i = \int_{l_i} f(x,y)\,dl. \tag{1}$$

Note that path l_i is a straight line connecting the i-th transmitter and receiver positions under the assumption of a straight propagation model. In this case, T_0 is related to the transmitter and receiver distance L as $T_0=L/c_0$. Based on the assumptions, the solution of eq.(1) is considered for obtaining the inverse sound velocity f in the medium from the observation data τ_i.

yamada@cc.tuat.ac.jp

2.2 Discretization of observation equation

We represent the image f on the continuous coordinates (x,y) with the sampled values f_j on the discrete grid points (x_j,y_j) (j=1,..,N) as

$$f(x,y) = \sum_{j=1}^{N} f_j \alpha_j(x,y), \tag{2}$$

where α_j is interpolation function.

By substituting eq.(2) into eq.(1), it can be rewritten in a discrete algebraic equations as,

$$\tau_i = \sum_{j=1}^{N} A_{ij} f_j, \tag{3}$$

where A_{ij} is the following matrix:

$$A_{ij} = \int_{l_i} \alpha_j(x,y)\,dl. \tag{4}$$

In this study, following Gaussian radial basis function (RBF) is used as an interpolation function:

$$\alpha_j(x,y) = \exp\left[-\frac{(x-x_j)^2+(y-y_j)^2}{2\sigma^2}\right], \tag{5}$$

where σ is a shape parameter of RBF.

2.3 Solution of algebraic equation

In the present problem, number of path M is extremely small compared to that of pixels N (i.e., $M \ll N$), moreover, part of the data passing through the spine is missing. Therefore, direct solution of eq.(3) cannot be obtained. To this end, the problem is replaced to the minimization of the following cost function J.

$$\arg\min_{f} J(\mathbf{f}) = (\boldsymbol{\tau}-\mathbf{A}\mathbf{f})^T(\boldsymbol{\tau}-\mathbf{A}\mathbf{f}) + \lambda \mathbf{f}^T\mathbf{f} \tag{6}$$

where $\boldsymbol{\tau}$ and $\mathbf{f}$ are the vectors with entity τ_i and f_j, respectively, $\mathbf{A}$ is matrix with entity A_{ij}, and subscript T denotes the transpose. The first term in the right-hand side of eq.(6) represents the error between observation data $\boldsymbol{\tau}$ and the calculated one with substitution $\mathbf{f}$ into the model equation (3). On the other hand, the second term is a regularization one to suppress the divergence of the solution. A regularization parameter λ determines the weight between the two. Starting from initial f_j^0, update calculation of eq.(7) is repeated until it converged to constant fixed value.

$$f_j^{k+1} = f_j^k + \mu\left(A_{ji}[p_i - (\mathbf{A}\mathbf{f}^k)_i] - \lambda f_j^k\right) \tag{7}$$

where the path number i is related to the iteration number k with $i=k$(mod M)+1 and μ is a parameter to control the speed of the convergence.

2.4 Determination of sound propagation path

The body surface data which is measured by laser range

sensor is used for the avoidance of the spine and determination of the sound propagation paths including the contact points of the transceivers on the body surface. Determination procedure is as shown in Fig.1. That is, the transceiver pair is translated along transverse direction with equal step Δx starting from right and left edges of the spine circle (Fig.1(b)). By this means, paths intersecting the spine area are avoided. The similar procedures are repeated until they are completed over the range between 0 and 180 degree with step $\Delta\theta$. Eventually, entire sound propagation paths were determined (Fig.1(c)).

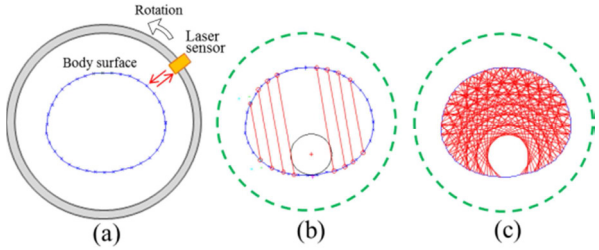

Fig.1 Determination of sound propagation path: (a) body surface data collected by the laser range sensor, (b) parallel translation paths avoiding the spine area, (c) entire paths after the iteration of the similar procedure at various rotated angle.

3 Test examination

3.1 Method

An abdominal numerical phantom (width: 420mm × height: 265mm) as shown in Fig.2 was prepared. The sound speeds in each areas, muscle, fat, intestine, etc., are as shown in the figure. The center position of the avoidance circle of the spine was set at the (-3 mm, -5 mm), and radius 50 mm. According to the method described in 2.4, sound propagation paths were determined. Where, maximum contact angle was set at ϕ_{max}=60 deg., angle step of rotation $\Delta\theta$=10 deg., translation step Δx=5mm, and total number of paths M=760. The travel time lag τ_i for each path was calculated based on the model eq.(1). The ART algorithm shown in 2.3 was applied to the simulation data. Objective square area with a side W=450 mm was set around the phantom, and discretized with N = 129x129 pixels. On that condition, inverse sound velocity image f_j was reconstructed.

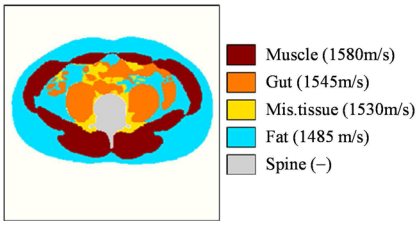

Fig.2 Abdominal numerical phantom.

3.2 Optimization of image reconstruction parameter

A. Control parameter μ By selecting the parameter μ between 0 and 1, iteration calculation of eq.(7) is known to converge in a fixed solution. When μ is selected closer to 1, convergent speed is fast, but at increased risk for converging in a divergent wrong solution. In opposite case of μ close to 0, it becomes a contrary situation. Taking these things into consideration, we selected μ at 0.05.

B. RBF interpolation parameter σ Reconstructed images are as shown in Fig.3, where RBF interpolation shape parameter $\tilde{\sigma}=\sigma/(\sqrt{2}W)$ is changed at three different values. As noted above μ is set at 0.05, and λ is set at 0.005 based on the later examination. For small value of $\tilde{\sigma}$=0.04, streak artifact is emerged due to the sparseness of the path. On the contrary, for large value of $\tilde{\sigma}$=0.16, definition of the image is deteriorated, instead of suppression of streak artifact. Eventually, for intermediate value of $\tilde{\sigma}$=0.1, image with reasonably high definition is obtained under the preventing condition of streak artefact generation.

C. Regularization parameter λ Under the fixed condition of μ=0.05 and $\tilde{\sigma}$=0.1, the reconstructed images are compared subject to the three different regularization parameters λ=0.0, 0.005 and 0.03, as shown in Fig.4. For small value of λ=0.0, accuracies of sound speed in each region are good but spotty artifacts are generated. On the contrary, for large value of λ=0.03, artifacts are suppressed, but contrast of sound speed is decreased. For intermediate value of λ=0.005, the results are obtained showing a good performance both for the accuracy of sound speed and the suppression of artifact.

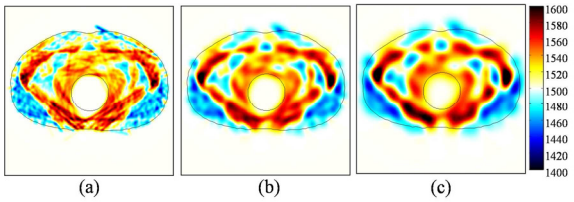

Fig.3 Reconstructed results for changing value of (a) $\tilde{\sigma}$=0.04, (b) $\tilde{\sigma}$=0.1, and (c) $\tilde{\sigma}$=0.16.

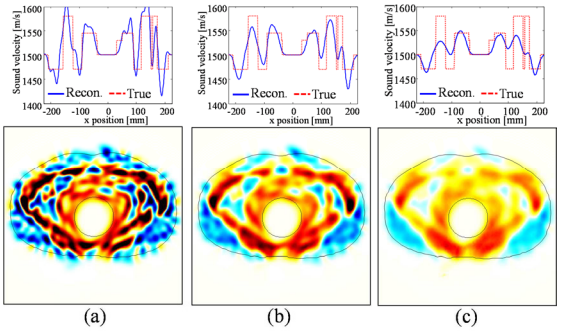

Fig.4 Reconstructed results for changing value of (a)λ=0.0, (b)λ=0.005, and (c)λ=0.03.

References

1. K. Nogami, A. Yamada, Jpn.J.Appl.Phys., 46, pp.4820-4826 (2007).
2. H.Li, D.Shimizu, T.Yokoyama and A.Yamada, Proc. Symp. Ultrasonic Electronics, 34, pp.493-494 (2013).
3. T. Yokoyama, D. Shimizu and A. Yamada, Proc. Symp. Ultrasonic Electronics, 35, pp.449-450(2014).